Geochemistry Geophysics Geosystems G3
AN ELECTRONIC JOURNAL OF THE EARTH SCIENCES
Published by AGU and the Geochemical Society

Article
Volume 2
December 18, 2001
Paper number 2001GC000152
ISSN: 1525-2027

Deep lithospheric dynamics beneath the Sierra Nevada during the Mesozoic and Cenozoic as inferred from xenolith petrology

Cin-Ty Lee
Division of Geological and Planetary Sciences, MC 170-25, California Institute of Technology, 1200 E. California Boulevard, Pasadena, California 91125, USA (ctlee@gps.caltech.edu)

Roberta L. Rudnick
Department of Geology, University of Maryland, College Park, Maryland 20742, USA (rudnick@geol.umd.edu)

George H. Brimhall Jr.
Department of Earth and Planetary Sciences, University of California, Berkeley, California 94720, USA (brimhall@socrates.berkeley.edu)

[1] **Abstract:** Peridotite xenoliths erupted in late Miocene basalts (~8 Ma) in the central Sierra Nevada sample a lithosphere that is vertically stratified in terms of age and thermal history. The deeper portions (~45–100 km) have asthenospheric osmium isotopic compositons and possess textural and chemical evidence for cooling from >1100° to 700–820°C. The shallower portions (<60 km) have unradiogenic Os isotopic compositions, which yield Proterozoic model ages, and contain orthopyroxenes that record temperatures as low as 670°C in their cores and heating up to 900°C on their rims. These observations suggest that the deeper xenoliths represent fragments of hot asthenosphere that upwelled to intrude and/or underplate the overlying Proterozoic lithosphere represented by the shallower xenoliths. The contrasting thermal histories between the shallow and deep xenoliths suggest that hot asthenosphere and cold lithosphere were suddenly juxtaposed, a feature consistent with the aftermath of rapid lithospheric removal or sudden intrusion of asthenospheric mantle into the lithosphere rather than passive extension. On the basis of regional tectonics and various time constraints, it is possible that this lithospheric removal event was associated with the generation of the Sierra Nevada granitic batholith during Mesozoic subduction of the Farallon plate beneath North America. Pleistocene basalt-hosted xenoliths record a different chapter in the geodynamic history of the Sierras. These xenoliths are relatively fertile, come from depths shallower than 45–60 km, are characterized by asthenospheric Os isotopic compositions, record hot equilibration temperatures (1000°–1100°C), and show no evidence for cooling. The strong contrast in composition and thermal history between the Pleistocene and late Miocene suites indicate that the post-Mesozoic lithospheric mantle, as represented by the latter, was entirely replaced by the former. The hot Pleistocene peridotites may thus represent new lithospheric additions associated with a post-Miocene lithospheric removal event or extension. High elevations, low sub-Moho seismic velocities, and the presence of fast velocity anomalies at 200 km depth may be manifestations of this event. If lithospheric removal occurred in the Mesozoic and Cenozoic, the observations presented here place constraints on the styles of lithospheric removal. In the Mesozoic, the lithospheric mantle was only partially removed, whereas in the Pliocene, the entire lithospheric mantle and probably the mafic lower crust were removed.

Keywords: Peridotite; delamination; Sierra; xenolith; osmium; lithosphere.

Index terms: Chemical evolution; Composition of the crust; Igneous petrology; Dynamics of lithosphere and mantle—general.

Received February 22, 2001; **Revised** August 2, 2001; **Accepted** August 31, 2001; **Published** December 18, 2001.

Lee, C.-T., R. L. Rudnick, and G. Brimhall, Deep lithospheric dynamics beneath the Sierra Nevada during the Mesozoic and Cenozoic as inferred from xenolith petrology, *Geochem. Geophys. Geosyst.*, 2, 10.1029/2001GC000152, 2001.

1. Introduction

[2] Lithospheric removal, defined here as any detachment, foundering, thermal erosion, or peeling away of the lithospheric mantle or lower crust into the convecting mantle (Figure 1), has been predicted by various geodynamic and conceptual theories [*Bird*, 1979, 1988; *Houseman et al.*, 1981; *Kay and Kay*, 1993; *Conrad and Molnar*, 1997; *Houseman and Molnar*, 1997]. The models predict that after cold lithosphere is replaced by hot asthenosphere, one would observe uplift, high elevations, low sub-Moho seismic velocities, and increased magmatism. In addition, a secular change in the isotopic composition of magmas might also be expected if their sources changed from old and enriched lithosphere to asthenosphere. However, many of these observations can also be explained by passive extension, which differs from lithospheric removal because it does not involve the return of lithospheric material to the convecting mantle.

[3] Determining whether or not lithospheric removal is a viable process has important geochemical implications. For example, lithospheric removal may be one means of recycling ancient lithospheric mantle and/or lower crust back into the convecting mantle. The former would give rise to enriched isotopic reservoirs within the convecting mantle, which may later be sampled by rising plumes [*McKenzie and O'Nions*, 1983]. The latter could explain why the continental crust is more evolved than mantle-derived melts; the lower crust tends to be mafic, and its removal would result in the net loss of mafic component from the crust [see *Rudnick*, 1995, and references therein].

[4] Here we use mantle xenoliths from a late Miocene basalt pipe and a Pleistocene basalt flow in order to constrain the thermal history and structure of the deep lithosphere beneath the extinct Sierra Nevada batholith at two points in its history. It has recently been suggested that the Sierran lithosphere has undergone two thinning events, once in the Mesozoic [*Lee et al.*, 2000] and once in the Pliocene [*Ducea and Saleeby*, 1998a, 1998b, 1998c]. Petrologic, thermobarometric, and isotopic data on the late Miocene and Pleistocene xenoliths are combined with thermal modeling in order to assess whether thinning was caused by passive extension or lithospheric removal.

2. Lithospheric Removal Mechanisms

[5] Lithospheric removal models are divided here into two groups, "mechanical" and "fluid", as shown schematically in Figure 1. Mechanical styles (Figures 1a–1c) either assume an intrinsic density instability that

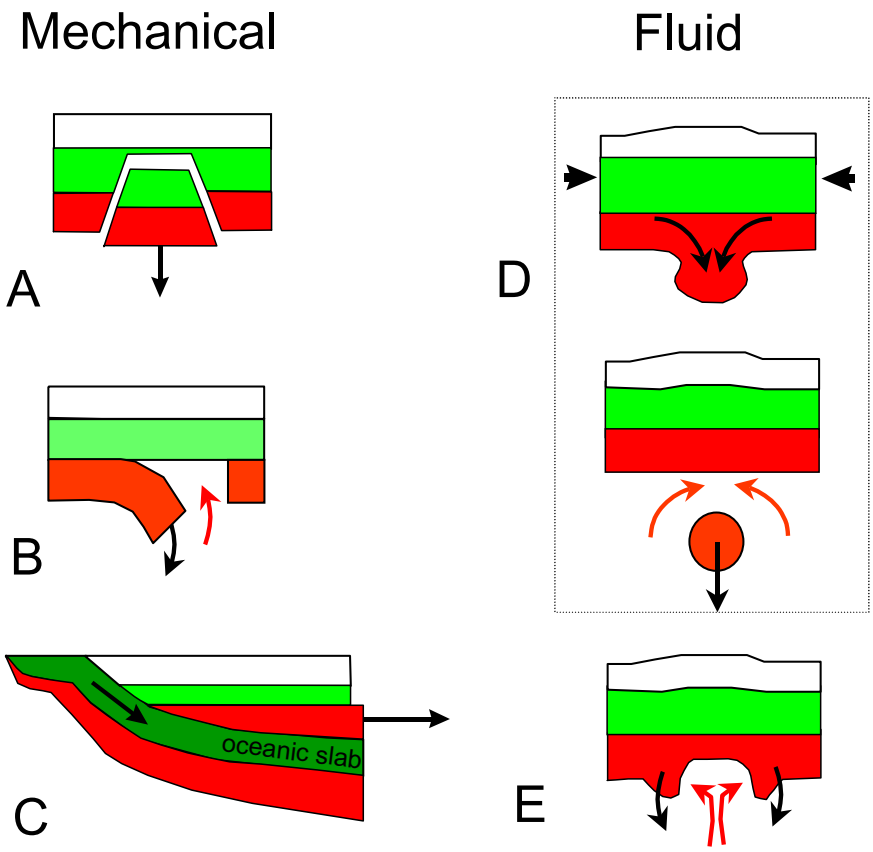

Figure 1. Lithospheric removal is defined herein to be any detachment, foundering, or peeling of the lithosphere (mantle and/or crust) into the convecting mantle. Scenarios for lithospheric removal can be subdivided into "mechanical" and "fluid" styles. The former involves (a) detachment, (b) peeling, or (c) shearing of the lithosphere at mechanical discontinuities (also known as "delamination"), such as the crust-mantle and mid-crustal boundaries. The latter invokes the growth of a density instability, modeled as an entirely fluid process rather than a mechanical process. Fluid processes of lithospheric removal could be in the form of (d) foundering or (e) thermal erosion.

results in peeling or detachment of the lithospheric mantle and/or lower crust from the overlying lithosphere [*Bird*, 1979], or remove the lithospheric mantle by coupling to a subducting oceanic plate [*Bird*, 1988]. These forms of lithospheric removal are also known as "delamination," and require some sort of mechanical discontuinity to allow for the decoupling and wholesale removal of lithosphere. Peeling or detachment presumably initiates within a weak layer, such as the midcrustal (Figure 1a) and crust-mantle (Moho, Figure 1b) boundaries, and propagation of delamination proceeds by the intrusion of hot asthenospheric mantle into a thin gap separating the crust from the lithospheric mantle (Figure 1c). In the second style of delamination, the lithospheric mantle is sheared away by coupling to a low-angle subducting oceanic slab. This style of delamination may have dictated Mesozoic and younger tectonics in the North American Cordillera, as several lines of evidence suggest that subduction of the Farallon plate beneath North America during

this time was at a shallow angle [*Dickinson and Snyder*, 1978].

[6] In the "fluid" styles of lithospheric removal, density perturbations derive from temperature contrasts, which are removed convectively [*Houseman et al.*, 1981; *Conrad and Molnar*, 1997; *Houseman and Molnar*, 1997] (we note that some of these models do not model the full convective equations but instead only model the growth of density perturbations, e.g., a Rayleigh-Taylor instability). For example, orogenic thickening of the thermal boundary layer depresses colder and hence denser mantle into the surrounding asthenosphere, leading to a dynamically unstable condition. If this density perturbation grows faster than it is thermally reequilibrated, foundering of the base of the thermal boundary layer occurs. The above-cited authors showed that the growth of these perturbations is superexponential in the case of power law rheology.

[7] "Fluid" models differ fundamentally from the "mechanical" models in that they do not predict wholesale removal of the lithospheric mantle or lower crust because, insofar as the mantle behaves like a fluid (without faults, necking, or other mechanical discontinuities), the lithospheric mantle would progressively thin rather than be completely removed during one event as suggested by the "mechanical" models of *Bird* [1979, 1988]. Also included in the "fluid" models is lithospheric removal by thermal erosion or subduction erosion, whereby anomalously hot asthenosphere in a plume or mantle wedge impinges against cold lithosphere, generating a convective instability.

[8] A feature common to all of these models of lithospheric removal is the rapidity (relative to thermal reequilibration) at which lithospheric removal proceeds, once initiated. All models predict lithospheric removal to occur over a time interval of 10–30 Ma, which is short relative to the timescales of thermal reequilibration (~100 Ma). The following thermal evolution is predicted [e.g., *Bird*, 1979; *Ranalli*, 1995, p. 366]. Immediately after lithospheric removal, hot asthenosphere passively rises to replace it. When the asthenosphere impinges the base of the remaining lithosphere, which is still cold because it has not had time to thermally reequilibrate, it cools, while what remains of the original lithosphere is heated (Figure 2a). Thus we predict that the lithosphere, reestablished after a lithospheric removal event, will be vertically stratified in terms of thermal history: the upper part will show heating, and the lower part will show cooling. As will be discussed later, if the original lithosphere is significantly older than the removal event, then the upper part will preserve ancient isotopic signatures, whereas the lower part will have younger isotopic signatures.

[9] Thermal erosion may also produce a similar thermal history because of the similar physical process involved in lithospheric removal (convection). From Figure 2b it can be seen that progressive thermal erosion results in the gradual heating of the overlying lithosphere during the lithospheric removal event. Figure 2b shows the case in which the upwelling asthenosphere is continually replenished so that it maintains a constant temperature. Eventually, however, the hot asthenosphere will cool and accrete to the overlying lithosphere, giving a stratification in thermal history similar to that seen after delamination, foundering, etc.

3. Extension

[10] *Jarvis and McKenzie* [1980] modeled the thermal evolution of lithosphere that is extended under pure shear strain (Figure 2c). In the simplest form of the model, the lithosphere, taken here to be equivalent to the thermal boundary layer, is instantaneously and

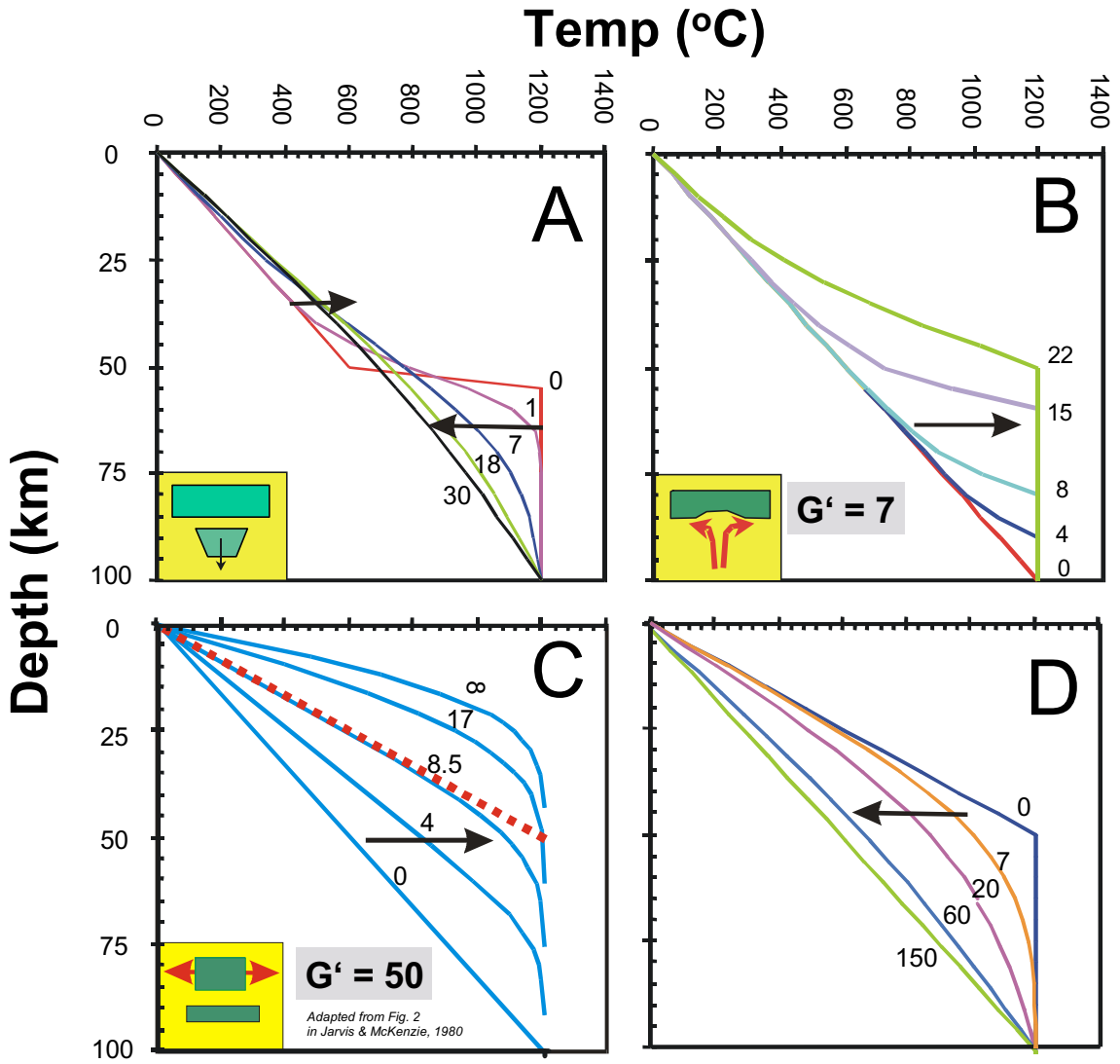

Figure 2. Thermal evolution of the lithosphere and/or underlying asthenosphere due to extension, and two types of lithospheric removal (thermal erosion and foundering/delamination). Numbers correspond to Ma and the thermal diffusivity used in all calculations is 10^{-6} m^2/s. (a) Thermal evolution of the lithosphere after lithospheric removal by foundering or delamination, using a finite difference method. Impingement of hot asthenosphere to the base of what remains of the original lithosphere results in cooling of the former and heating of the latter. (b) Simplified thermal evolution of the lithosphere during thermal erosion, modeled using a finite-difference method. A low Peclet number, G', is used to emphasize that the lithosphere is progressively being heated (in this case, the lithosphere is assumed to be 100 km thick and the upward velocity of upwelling mantle is 0.2 cm/yr). For higher Peclet numbers, heating of the uppermost part of the lithosphere would be dampened. (c) Thermal evolution of lithosphere during pure shear, modified from Figure 2 by *Jarvis and McKenzie* [1980] for $G' = 50$ (upward velocity of base of lithosphere is 1.5 cm/yr). Red line represents the condition where $G' = \infty$ and where $\beta = 2$, i.e., when the lithosphere is instantaneously stretched by a factor of 2. (d) Reequilibration of the lithosphere thinned by $\beta = 2$. Note that thermal reequilibration of lithosphere thinned by active upwelling or extension results in cooling in both the original lithosphere and the underlying asthenosphere.

homogeneously extended by a factor of β. As a result, the geothermal gradient increases by a factor of β, while hot asthenospheric mantle passively upwells to fill the region created by lithospheric thinning (localized heating associated with intrusion of basaltic magmatism is ignored for simplicity). If the rate of extension is finite, then the evolution of the lithospheric geotherm depends on the balance between the rate of extension and the rate of thermal reequilibration, quantitatively expressed as the Peclet number, $G' = aV/\kappa$, where a represents the thickness of the lithosphere, V represents the vertical velocity at the base of the lithosphere, and κ represents the thermal diffusivity. Finite Peclet numbers result in convex upward geotherms; steady state temperature profiles are shown in Figure 2c. For most geologically reasonable Peclet numbers, the increase in average geothermal gradient can be approximated by instantaneous stretching, i.e., $G' = \infty$. During extension, the lithosphere undergoes progressive heating, and hot asthenosphere passively rises to fill the growing gap, so that neither the lithosphere nor the asthenosphere should show evidence for significant cooling during extension. However, as soon as extension ends or slows down, the geotherm returns to equilibrium by conductive cooling. In so doing, the thermal boundary layer returns to its original thickness by incorporating part of the convecting asthenosphere. Importantly, during thermal reequilibration, both the original lithosphere and the incorporated asthenosphere will cool (Figure 2d).

4. A Case Study of Deep Lithospheric Dynamics Beneath the Sierra Nevada

4.1. Evidence for Mesozoic and Cenozoic Thinning of the Lithosphere

[11] The Sierra Nevada, an extinct Mesozoic arc, located on the western edge of the North American continent, is a region where much circumstantial evidence suggests that the lithospheric mantle has been thinned both in the Mesozoic and in the Cenozoic (Figure 3). *Ducea and Saleeby* [1996, 1998a, 1998b] outline the following lines of evidence for thinning in the late Cenozoic. The highest elevations in the Sierra Nevada (eastern Sierras) are underlain by anomalously thin crust, implying that the elevations must be sustained by low-density material beneath the crust, such as hot asthenospheric mantle [*Jones et al.*, 1994; *Wernicke et al.*, 1996]. This interpretation is supported by the presence of low sub-Moho seismic velocities beneath the Sierra Nevada [*Ruppert et al.*, 1998]. In addition, there has been an insurgence of alkalic volcanism in the Sierra Nevada, as well as on its flanks, since the late Miocene [*Moore and Dodge*, 1980]. Older lavas have enriched isotopic signatures (Nd and Sr), whereas younger lavas have depleted signatures, suggesting a change from lithospheric to asthenospheric sources [*Farmer et al.*, 1989]. It has also been suggested that older lavas have a deeper source than younger lavas, indicating progressive thinning of the lithosphere [*Feldstein and Lange*, 1999]. *Ducea and Saleeby* [1996] reported that late Miocene basalts contain abundant garnet-bearing lower crustal xenoliths, while late Pliocene and younger basalts lack garnet-bearing xenoliths altogether. This observation may suggest that the Sierran lower crust was removed sometime after the Miocene [*Ducea and Saleeby*, 1996]. High seismic velocities beneath the western and southern portions of the Sierra Nevada at depths greater than 150 km have been interpreted to represent downwelling portions of the lithosphere [*Jones et al.*, 1994; *Zandt and Carrigan*, 1994].

[12] *Lee et al.* [2000] reported asthenospheric Os isotopic ($^{187}Os/^{188}Os = 0.122 - 0.131$) compositions for the majority of peridotite xenoliths from both late Miocene and Pleistocene basalts erupted through the central and

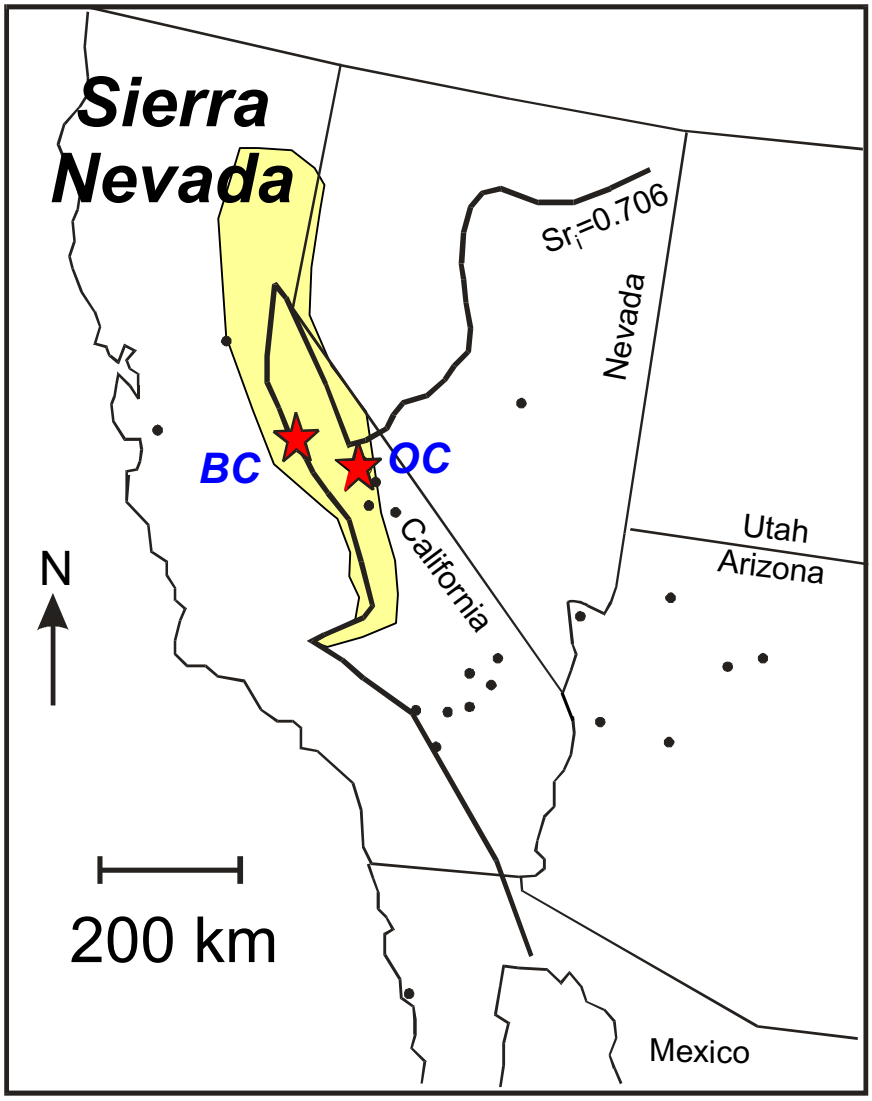

Figure 3. Map of the Sierra Nevada showing the two xenolith localities, Big Creek and Oak Creek. Both sites are located east of the initial $^{87}Sr/^{86}Sr$ ratio contour (Sr_I) in granitic rocks of the Sierran batholith. This contour is generally taken to represent the western edge of the Precambrian craton [*Kistler*, 1990].

eastern Sierra Nevada but found Proterozoic model ages for the shallowest peridotites erupted in the Miocene. Because this region of the Sierra Nevada is underlain by juvenile Proterozoic crust, it must have once been underlain by Proterozoic lithospheric mantle, as sampled by the shallowest Miocene-hosted xenoliths. Lee et al. interpreted the asthenospheric Os isotopic compositions of the deeper xenoliths to indicate that most of the ancient lithospheric mantle was already removed or thinned by the late Miocene.

Table 1. Orthopyroxene Compositions

	Big Creek Xenoliths									
	P-1[a]		P-2[a]	P-6[b]		P-7		P-10[b]		
	Core	Rim	Unzoned	Core	Rim	Core	Rim	Core	Rim	Core of Large opx
SiO_2	54.36	55.88	56.93	54.70	57.42	53.96	54.85	54.80	55.61	54.14
TiO_2	0.14	0.10	0.04	0.09	0.06	0.14	0.07	0.09	0.08	0.06
Al_2O_3	4.37	2.28	1.50	5.23	1.03	4.46	3.69	3.08	2.50	3.08
Cr_2O_3	0.35	0.18	0.16	0.39	0.13	0.47	0.40	0.55	0.46	0.55
FeO	7.52	7.78	5.64	6.57	6.47	6.56	6.50	6.05	6.18	6.02
MnO	0.20	0.20	0.17	0.12	0.15	0.14	0.16	0.14	0.16	0.14
MgO	32.23	33.34	34.84	32.69	34.87	32.73	33.86	33.53	34.05	33.52
CaO	0.73	0.27	0.18	0.53	0.20	0.78	0.19	0.49	0.29	0.72
Na_2O	0.02	0.02	0.02	0.06	0.01	0.05	0.03	0.05	0.02	0.04
Total	99.92	100.05	99.48	100.37	100.35	99.30	99.72	98.79	99.34	98.26
Mg/(Mg + Fe)	0.884	0.884	0.917	0.899	0.906	0.899	0.903	0.908	0.908	0.909

[a]Data taken from *Mukhopadhyay and Manton* [1994].
[b]Garnet-bearing.

[13] In this paper, we present petrologic and thermobarometric data, which, when used in conjunction with the previously reported Os isotopic data, allow the vertical structure and thermal history of the Sierran lithosphere to be determined. By comparing these results to thermal models for various forms of lithosphere removal, we are able to speculate on the causes of lithospheric removal beneath the Sierras.

4.2. Thermal Histories Recorded in Xenoliths

[14] We examined xenoliths from two localities in the Sierra Nevada (Figure 3). The first xenolith suite comes from the late Miocene (8.3 Ma) Big Creek diatreme, which erupted in the central Sierra Nevada, slightly west of the crest. The second suite comes from the Oak Creek flow, associated with the Pleistocene Big Pine volcanic field (~0.115 Ma) in the eastern Sierras and on the west flank of the Owens Valley. Outcrops of the Oak Creek basalts are actually remnants, now perched on canyon walls, of a larger flow that originated somewhere in the high Sierras. Although both suites contain mantle xenoliths, garnet-bearing lower crustal xenoliths (garnet clinopyroxenites and garnet websterites) and garnet-bearing peridotites occur only at Big Creek. The garnet clinopyroxenites have been the focus of much study by *Mukhopadhyay and Manton* [1994] and *Ducea and Saleeby* [1996, 1998a, 1998c]. The Miocene-hosted peridotite xenoliths have been previously described by *Dodge et al.* [1988] and Mukhopadhyay and Manton, but only brief descriptions of their thermal histories have been reported. Here we focus on detailed petrographic and thermobarometric analyses of peridotite xenoliths from both sites. As summarized below, there are fundamental differences between peridotite xenoliths from these two sites. Mineral compositions and thermobarometry are given in Tables 1-6.

4.2.1. Peridotites from the Late Miocene Big Creek diatreme

[15] Peridotite xenoliths at Big Creek range from lherzolites to harzburgites, indicating that they experienced variable degrees of melt depletion. This is evidenced by olivine forster-

Table 1. (continued)

Big Creek Xenoliths								Oak Creek Xenoliths			
D-18[b]		BC98-2		BC77[b]		1026V[b]		OK98-2	OK98-3	OK98-4	OK98-9
Core	Rim	Core	Rim	Core	Rim	Core	Rim				
56.37	57.01	57.61	57.04	56.24	56.42	55.23	58.09	55.12	53.76	54.33	54.17
0.13	0.06	0.02	0.01	0.04	0.02	0.03	0.02	0.13	0.19	0.14	0.14
1.95	1.07	0.66	2.12	1.66	1.54	3.18	0.73	3.45	5.36	4.82	5.12
0.31	0.22	0.11	0.15	0.34	0.39	0.38	0.18	0.52	0.37	0.30	0.29
6.30	5.90	5.64	5.60	5.66	5.74	5.64	5.47	6.27	6.67	6.50	6.59
0.12	0.10	0.11	0.14	0.11	0.13	0.11	0.12	0.13	0.16	0.14	0.16
34.11	35.23	36.07	34.68	34.84	35.09	33.92	35.93	33.35	32.57	32.95	33.01
0.43	0.19	0.11	0.46	0.40	0.10	1.01	0.13	0.88	0.93	0.83	0.85
0.05	0.03	0.02	0.03	0.03	0.01	0.25	0.00	0.08	0.11	0.11	0.09
99.77	99.81	99.82	100.22	99.32	99.44	99.75	100.67	99.93	100.12	100.11	100.42
0.906	0.914	0.937	0.917	0.916	0.916	0.915	0.921	0.905	0.897	0.900	0.899

ite (Fo) contents (Mg # = molar Mg/(Mg + Fe)) ranging from 0.886 (fertile) to 0.914 (depleted), and negative correlations between olivine forsterite content and the amount of TiO_2 and Na_2O in clinopyroxene (Figure 4). We selected five spinel peridotites and four garnet-bearing spinel peridotites for thermobarometric and Re-Os isotopic work.

[16] Big Creek xenoliths can be subdivided into two categories, one group that shows textural and chemical evidence for cooling (n = 7 samples) and a second group that shows no evidence for cooling (n = 2). The former includes both garnet-bearing and spinel peridotites, whereas the latter consists strictly of spinel peridotites that record the lowest equilibration temperatures of the entire peridotite xenolith suite. Combined with the lack of garnet, this suggests that the second group of xenoliths derive from shallower depths than the first, implying a lithosphere that may be vertically stratified in terms of its thermal history. We assume that the observed thermal histories are not related to the eruption event that brought the xenoliths to the surface because only one of the shallow xenoliths shows evidence for heating and most (the deeper xenoliths) show only cooling.

4.2.1.1. Late Miocene peridotites with evidence for cooling

[17] All garnet-bearing peridotites from Big Creek show evidence for cooling: spinels rimmed by garnet coronae and orthopyroxenes and clinopyroxenes containing garnet exsolution lamellae (Figure 5), which indicate that the samples crossed into the garnet stability field. Although this may occur in response to increased pressure or decreased temperature, we believe the latter is responsible, given the temperatures recorded by zoned minerals. Unexsolved cores of orthopyroxenes in the garnet peridotites have high Ca, while those portions of orthopyroxenes that have exsolved garnet have low Ca (Figure 6). Final recorded temperatures, based on garnet-pyroxene lamellae, range from 760° to 900°C [*Harley*, 1984], approaching the temperatures of the cold peridotites described in section 4.2.1.2. Peak temperatures (900°–1140°C, Figure 7) are

Table 2. Clinopyroxene Compositions

	Big Creek Xenoliths												Big Creek Xenoliths			Oak Creek Xenoliths			
	P-1[a]	P-2[a]	P-6[b]		P-7		P-10		D-18[b]		BC98-2		BC77[b]	1026V[b]		OK98-2	OK98-3	OK98-4	OK98-9
			Core	Rim	Core	Rim	Core	Rim	Core	Rim	Core	Rim		Core	Rim				
SiO_2	53.28	55.24	53.81	54.47	52.03	52.73	50.79	52.81	53.96	53.87	54.48	52.32	53.66	52.22	53.70	51.84	51.05	51.29	51.05
TiO_2	0.30	0.05	0.48	0.29	0.39	0.28	0.47	0.22	0.33	0.24	0.03	0.03	0.05	0.07	0.07	0.40	0.65	0.59	0.61
Al_2O_3	2.80	1.43	3.69	2.78	4.76	3.29	5.84	2.53	3.30	2.41	1.17	3.88	1.37	4.02	2.00	4.75	7.64	7.29	7.32
Cr_2O_3	0.52	0.33	0.57	0.56	0.91	0.68	0.98	1.04	0.78	0.88	0.58	0.67	0.79	0.95	0.96	1.19	0.72	0.69	0.58
FeO	2.22	1.65	2.32	2.33	2.07	2.22	2.57	1.89	2.13	2.21	1.61	2.69	2.45	2.69	1.91	3.13	3.70	3.23	3.71
MnO	0.10	0.08	0.08	0.07	0.07	0.07	0.07	0.10	0.07	0.07	0.07	0.10	0.07	0.12	0.07	0.09	0.11	0.09	0.13
MgO	16.62	17.08	15.52	16.05	15.13	15.95	16.32	16.41	15.79	16.28	17.44	18.08	16.89	17.55	16.89	16.45	14.93	15.20	15.38
CaO	23.65	23.04	21.57	22.02	21.82	22.20	19.55	23.15	21.87	22.57	23.51	20.66	22.65	20.47	22.51	20.22	18.97	19.25	19.33
Na_2O	0.54	0.56	1.63	1.44	1.41	1.00	1.49	0.70	1.52	1.24	0.64	0.38	0.88	0.83	0.98	1.04	1.67	1.76	1.63
Total	100.00	99.46	99.66	100.03	98.58	98.42	98.08	98.86	99.74	99.76	99.53	98.82	98.81	98.92	99.09	99.11	99.44	99.37	99.72
Mg/(Mg + Fe)	0.930	0.949	0.923	0.925	0.929	0.928	0.919	0.939	0.930	0.929	0.951	0.923	0.925	0.921	0.940	0.904	0.878	0.894	0.881

[a]Data taken from *Mukhopadhyay and Manton* [1994].
[b]Garnet-bearing.

Table 3. Olivine Compositions

	Big Creek Xenoliths						Big Creek Xenoliths			Oak Creek Xenoliths			
	P-1[1]	P-2[1]	P-6[2]	P-7	P-10	D-18[2]	BC98-2	BC77[2]	1026V[2]	OK98-2	OK98-3	OK98-4	OK98-9
SiO_2	40.50	41.00	40.10	40.36	40.01	39.84	40.60	39.89	40.34	40.18	40.41	40.17	40.19
TiO_2	0.00	0.00	0.00	0.01	0.03	0.02	0.01	0.00	0.01	0.00	0.00	0.01	0.00
Al_2O_3	0.00	0.00	0.01	0.02	0.01	0.02	0.02	0.01	0.01	0.03	0.04	0.03	0.03
Cr_2O_3	0.00	0.00	0.00	0.02	0.00	0.02	0.01	0.00	0.03	0.02	0.00	0.01	0.02
FeO	11.00	8.39	9.63	9.66	8.69	9.44	8.48	8.64	8.80	9.68	10.22	9.70	10.16
MnO	0.14	0.12	0.09	0.12	0.16	0.11	0.14	0.10	0.10	0.15	0.17	0.17	0.14
MgO	47.90	50.10	49.35	49.14	48.71	48.36	49.92	49.37	49.70	48.96	48.50	48.68	48.90
NiO	0.32	0.41	0.38	0.37	0.37	0.36	0.45	0.40	0.37	0.36	0.37	0.40	0.34
CaO	0.01	0.01	0.01	0.01	0.02	0.01	0.03	0.01	0.01	0.08	0.07	0.07	0.09
Total	99.87	100.03	99.57	99.69	97.98	98.16	99.75	65.81	99.35	99.43	99.78	99.21	99.86
Mg/(Mg + Fe)	0.886	0.914	0.901	0.901	0.909	0.901	0.913	0.911	0.910	0.900	0.894	0.900	0.896

[1]Data taken from *Mukhopadhyay and Manton* [1994].
[2]Garnet-bearing.

Table 4. Spinel Compositions

	Big Creek Xenoliths							Big Creek Xenoliths			Oak Creek Xenoliths			
	P-1[a]	P-2[a]	P-6[b]	P-7	P-10	D-18[b]	BC98-2	BC77[b]	1026V[b] (2ndry)	1026V[b] (2ndry)	OK98-2	OK98-3	OK98-4	OK98-9
TiO_2	0.09	0.07	0.42	0.07	0.22	0.59	0.17	0.31	0.36	0.00	0.35	0.16	0.16	0.16
Al_2O_3	52.4	30.15	29.74	51.71	36.64	24.93	19.47	31.31	17.59	58.72	40.86	58.01	57.79	59.28
Cr_2O_3	12.00	33.71	33.88	15.06	27.94	37.42	49.23	32.38	44.37	8.40	25.08	8.22	9.13	7.52
V_2O_5	-	-	0.26	0.09	0.20	0.41	0.29	0.33	0.38	0.03	0.20	0.09	0.12	0.06
FeO	18.42	16.58	21.99	15.24	21.25	26.16	14.69	19.81	24.98	11.39	15.45	12.72	11.98	12.37
MnO	0.18	0.18	0.35	0.14	0.25	0.38	0.25	0.20	0.26	0.18	0.16	0.07	0.08	0.09
MgO	16.78	16.32	12.90	17.69	13.92	10.25	15.64	14.45	10.87	20.38	18.25	20.91	20.85	21.04
NiO	-	-	0.15	0.29	0.18	0.17	0.21	0.24	0.10	0.23	0.33	0.38	0.38	0.43
ZnO	-	-	0.11	0.10	0.12	0.23	0.03	0.10	0.10	0.01	0.02	0.06	0.05	0.03
Total	100.29	98.33	99.83	100.38	100.69	100.56	100.14	99.20	99.05	99.34	100.79	100.68	100.57	101.03
Cr/(Cr + Al)	0.133	0.429	0.433	0.163	0.338	0.502	0.629	0.410	0.629	0.088	0.292	0.087	0.096	0.078

[a]Data taken from *Mukhopadhyay and Manton* [1994].
[b]Garnet-bearing.

Table 5. Garnet Compositions

	Big Creek Xenoliths			
	P-6	D-18	BC77	1026V
SiO_2	41.63	42.00	41.18	41.89
TiO_2	0.10	0.16	0.02	0.03
Al_2O_3	23.26	22.64	22.18	22.44
Cr_2O_3	0.68	1.45	1.44	1.65
FeO	9.67	9.53	9.07	9.52
MnO	0.45	0.44	0.46	0.48
MgO	19.55	19.15	19.71	19.22
CaO	4.70	5.12	4.50	5.17
Total	100.04	100.48	98.56	100.40

recorded in unexsolved portions of orthopyroxenes by the Ca-in-Opx thermometer [*Brey and Kohler*, 1990]. In addition, orthopyroxenes are zoned in Al and Ca toward clinopyroxene contacts (Figures 7 and 8). Rim temperatures of zoned Opx range from 700° to 820°C. More confidence is placed in temperatures based on the Ca content of single orthopyroxene grains than on temperatures based on mineral pairs (e.g., garnet-pyroxene and clinopyroxene-orthopyroxene Mg-Fe exchange thermometers), as mineral heterogeneity limits the accuracy of mineral pair thermometry (see Table 6).

[18] Evidence for cooling is also seen in most of the spinel peridotites (section 4.2.1.2 describes the two samples that do not show cooling). These possess clinopyroxenes and orthopyroxenes with fine pyroxene exsolution lamellae (orthopyroxene and clinopyroxene, respectively). Orthopyroxenes are zoned from high Ca cores to low Ca rims in contact with clinopyroxene (Figures 6 and 7), while clinopyroxenes are zoned from low Ca cores to high Ca rims. Peak temperatures (cores) are as high as 1050°C. The lowest Ca-in-orthopyroxene temperature (rim) recorded by these xenoliths is 750°C.

[19] Equilibration pressures calculated for the garnet-bearing peridotites (using garnet-orthopyroxene lamellae pairs) range from 2.7 to 3.3 GPa [*Brey and Kohler*, 1990], corresponding to depths of ~70 and ~100 km (Figure 9). Equilibration pressures cannot be determined for spinel peridotites owing to the lack of well-calibrated barometers. However, a maximum pressure constraint can be determined by the absence of garnet and from calibrations of the spinel-garnet transition as a function of Cr content in spinels [*O'Neill*, 1981]. For the Cr contents of these spinels (Cr/(Cr + Al) = 0.3–0.7), maximum pressures are ~2.5–3 GPa. This pressure range coincides with pressures calculated for garnet websterite xenoliths from Big Creek [*Ducea and Saleeby*, 1998c]. Garnet websterites may be cumulates or restites associated with the formation of the Sierra Nevada batholith [*Ducea and Saleeby*, 1998c], and therefore the overlap in pressures suggest that the garnet and spinel peridotites studied here are interleaved with garnet websterites.

4.2.1.2. Late Miocene peridotites with no evidence for cooling

[20] Two of the Big Creek peridotites we originally selected for Re-Os isotopic analyses show no evidence for cooling (P2 and BC98-2). Both of these are refractory (Fo = 0.913–0.914) spinel peridotites. Orthopyroxenes in P2 are unzoned (according to *Mukhopadhyay and Manton* [1994]; unfortunately, owing to limited

Table 6. Thermobarometry[a]

	Temperature, °C				P, GPa	
	Input P, GPa	cpx-opx	CaO in opx	gt-opx	BKN	HG
Big Creek, Garnet-Bearing						
1026V						
opx core	3		1140			
opx rim	3		730			
cpx-opx core	3	1110				
cpx-opx rim	3	800				
gt-opx				790		2.9
gt-opx				810	3.3	
BC77						
opx core	3		920			
opx rim	3		700			
gt-opx				830		2.3
gt-opx				800	3.2	
P6						
core cpx-opx	3	800				
core cpx-opx	3	790				
opx core	3		930			
opx rim	3		800			
gt-cpx	3			920		
gt-opx				931	3.5	
gt-opx		780			2.7	
gt-opx				910		3.1
D18						
cpx-opx core	2	740				
cpx-opx rim	2	700				
opx core	3		930			
opx rim	3		790			
gt-opx				830	2.8	
gt-cpx	3					
gt-opx				820		2.6
Big Creek, Spinel Peridotites						
P1						
opx core	2		1000			
opx rim	2		806			
opx-cpx	2	720				
P2						
opx ave	2		740			
opx-cpx ave	2	859				
P7						
opx core	2		1020			
opx rim	2		750			
opx-cpx core	2	760				
opx-cpx rim	2	800				
P10						
opx core	2		920			
large opx core	2		1000			
opx rim	2		820			
opx-cpx core	2		1050			
opx-cpx rim	2		710			
BC98-2						
opx core	2		670			
opx-cpx core	2		720			

Table 6. (continued)

	Temperature, °C				P, GPa	
	Input P, GPa	cpx-opx	CaO in opx	gt-opx	BKN	HG
opx rim	2		900			
opx-cpx rim	2		1100			
			Oak Creek			
OK98-2	2	1080	1050			
OK98-3	2	1090	1060			
OK98-4	2	1070	1030			
OK98-9	2	1080	1040			

[a]Temperatures, cpx-opx [*Brey and Kohler*, 1990]; CaO in opx [*Brey and Kohler*, 1990]; gt-opx [*Harley*, 1984]. Pressures based on Al solubility in opx coexisting with gt, BKN [*Brey and Kohler*, 1990], HG [*Harley and Green*, 1982]; temperature calculations require an input pressure. In the case of garnet-bearing peridotites, a thermometer and barometer can be solved simultaneously to yield a unique *P* and *T* (calculations based on garnet and pyroxene rims).

sample size, we did not have a polished section of this sample), whereas orthopyroxenes in BC98-2 appear to be enriched in Ca on the rims, indicating heating (Figures 6–8). Importantly, the core Ca-in-orthopyroxene temperatures recorded in both of these xenoliths are the lowest in the entire xenolith suite, yielding temperatures of 670° and 740°C for BC98-2 and P2, respectively. The low equilibration temperatures and the lack of garnet suggest derivation from shallower depths (<45–60 km) than those xenoliths that show cooling. The slightly enriched Ca rim of the orthopyroxenes in BC98-2 suggest heating up to 900°C. Interestingly, orthopyroxenes in one of the peridotites (BC8) studied by *Mukhopadhyay and Manton* [1994] record similar Ca zonation to BC98-2. BC8's core also records an extremely low Ca in orthopyroxene temperature (704°C), whereas its rim records heating up to 805°C, and like the samples described above, it is also very refractory (Fo = 0.914). Unfortunately, BC8 was not available for Re-Os isotopic analysis.

4.2.2. Pleistocene Oak Creek Peridotites

[21] Oak Creek peridotites are exclusively spinel lherzolites; no garnet-bearing peridotites have been reported (Fe-rich dunites and wehrlites also occur, but we interprete them as magmatic cumulates and do not discussed them here). These peridotites are distinct from Big Creek peridotites in several ways: (1) Oak

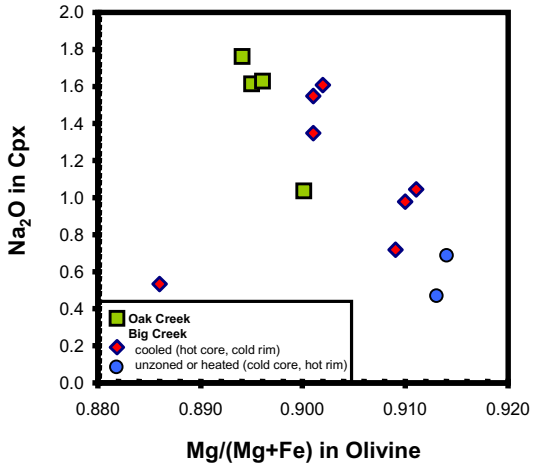

Figure 4. Na_2O in clinopyroxene versus Mg/(Mg + Fe) in olivine. The negative correlation is consistent with the incompatibility of Na and compatibility of Mg during partial melting. The one sample that plots off the trend (P-1) has spinel with low Cr/Cr + Al (0.13), consistent with the low Mg/(Mg + Fe) in olivine, which indicates that this sample has had only minor amounts of partial melt extracted from it. The low low Na_2O in the clinopyroxene may thus indicate some recent disturbance to the clinopyroxene.

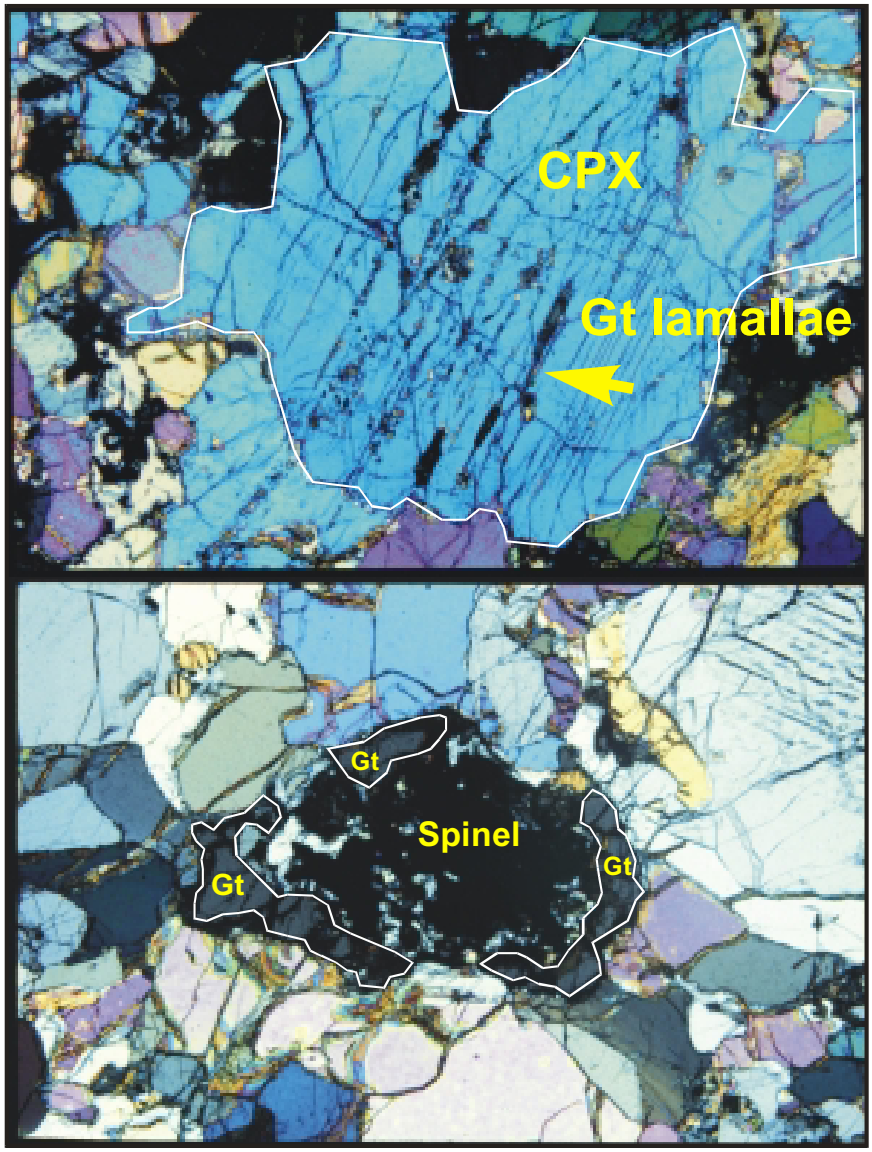

Figure 5. Textural evidence for cooling in Big Creek xenoliths (sample 1026V, which exhibits the highest Opx CaO content of the suite). (top) Garnet exsolution lamellae (opaque) in clinopyroxene under crossed polars. Clinopyroxene grain is ~2 mm in diameter. (bottom) Spinel (opaque) rimmed by garnet (isotropic) under crossed polars. Diameter of garnet-spinel corona is ~1 mm. Final recorded temperatures and pressures are calculated from microprobe analyses near garnet-pyroxene contacts or from clinopyroxene-orthopyroxene contacts. "Peak" temperatures are determined from the CaO content of the cores or least exsolved portions of orthopyroxenes.

Creek peridotites are restricted to relatively fertile compositions (Mg # = 0.89–0.90), indicating lesser degrees of partial melt extraction (Figure 4); (2) they do not show chemical or textural evidence for disequilibria (e.g., Figures 5 and 6); (3) temperatures based on the Ca content of single orthopyroxene grains are within error of those based on Mg-Fe exchange

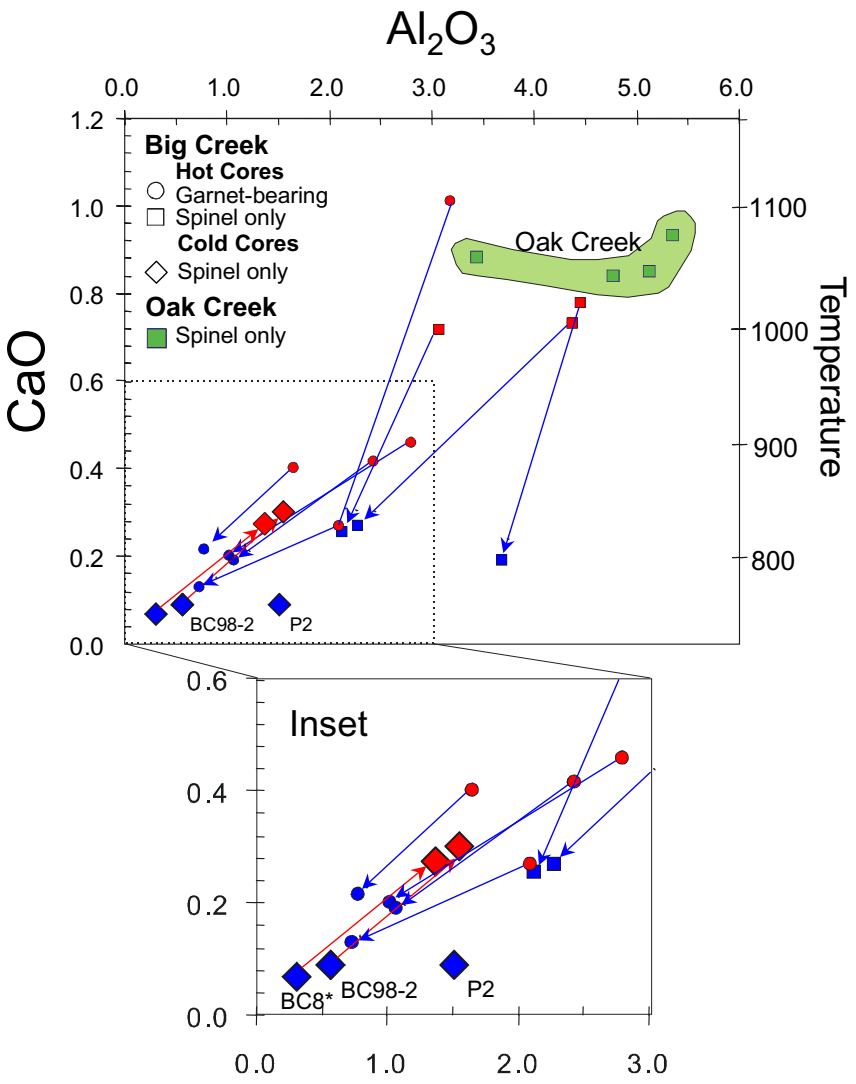

Figure 6. Orthopyroxenes in many of the Big Creek xenoliths are zoned in terms of CaO and Al_2O_3. Tie lines connect core compositions to rim compositions (arrows point to rims). P2 does not have tie lines and represents unzoned orthopyroxene. Note that those with the lowest CaO cores (hence lowest equilibration temperatures) are either unzoned or show heating (high Ca rim), whereas Big Creek orthopyroxenes with high CaO cores all show cooling (low Ca rim). Also, note the homogeneity in CaO content of orthopyroxenes in Oak Creek peridotites. The equivalent temperature (approximate) for a given CaO content in orthopyroxene is shown on the right-hand axis. Data for sample BC8 are taken from *Mukhopadhyay and Manton* [1994] but were not available for this study.

between clinopyroxene and orthopyroxene, illustrating attainment of equilibrium in Oak Creek minerals; (4) equilibration temperatures for all of the xenoliths fall within 1000°–1100°C and are considerably hotter than the final temperatures recorded by the Big Creek xenoliths (Figure 9; these temperatures are consistent with those calculated by *Ducea and Saleeby* [1996]); and (5) Oak Creek spinels have low Cr contents, thus maximum pressures for these xenoliths are

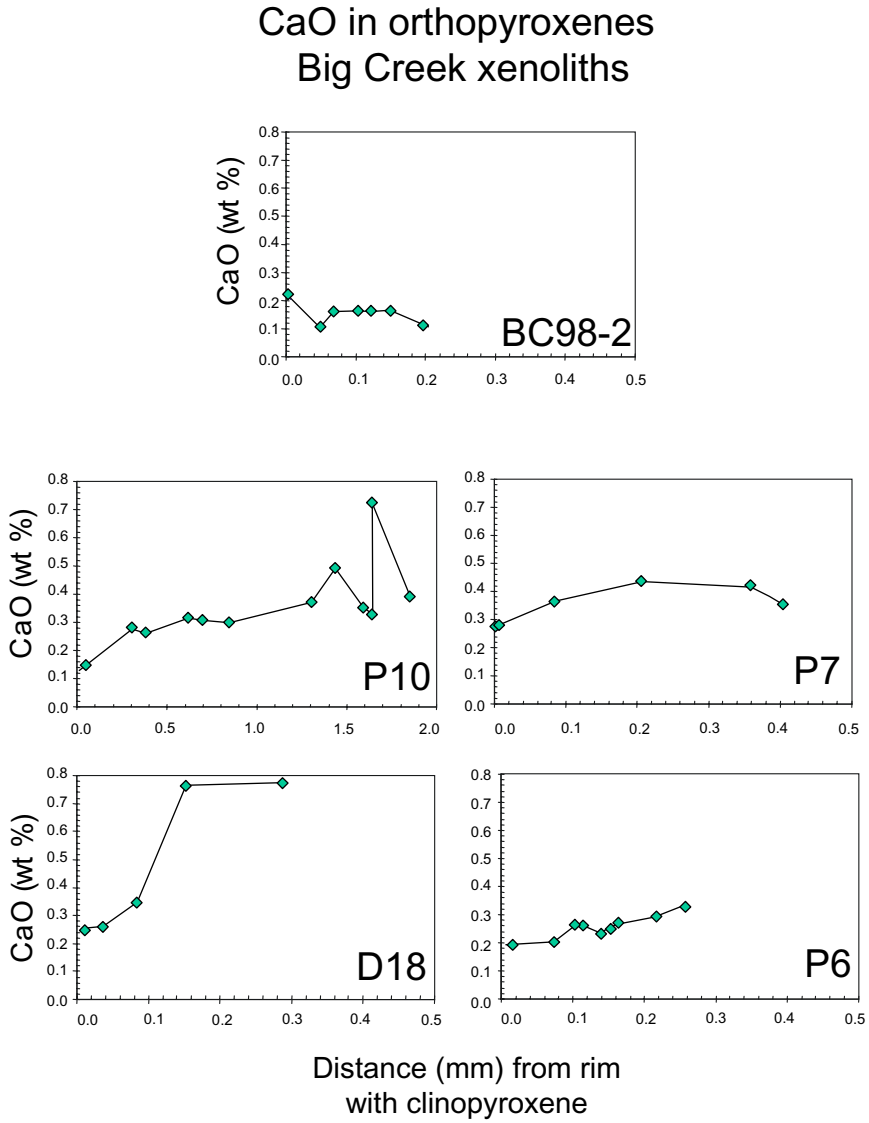

Figure 7. CaO content of orthopyroxene as a function of distance (mm) away from contact with clinopyroxene in Big Creek xenoliths.

between 1.5 and 2 GPa, or ~45–60 km depth and are therefore shallower than the garnet-bearing Big Creek peridotites.

4.3. Re-Os Isotopic Systematics

[22] Re-Os isotopic systematics [*Lee et al.*, 2000] show that the deep peridotites from the Miocene Big Creek pipe have $^{187}Os/^{188}Os$ between 0.1263 and 0.1296 (excluding 1026V, which has a super-chondritic ratio), and lie within the range of modern day asthenospheric $^{187}Os/^{188}Os$ (0.122–0.130; see *Lee et al.* [2000] for discussion). Combined with the fact that these peridotites exhibit a range in Mg # and Na_2O in clinopyroxene (hence a wide range

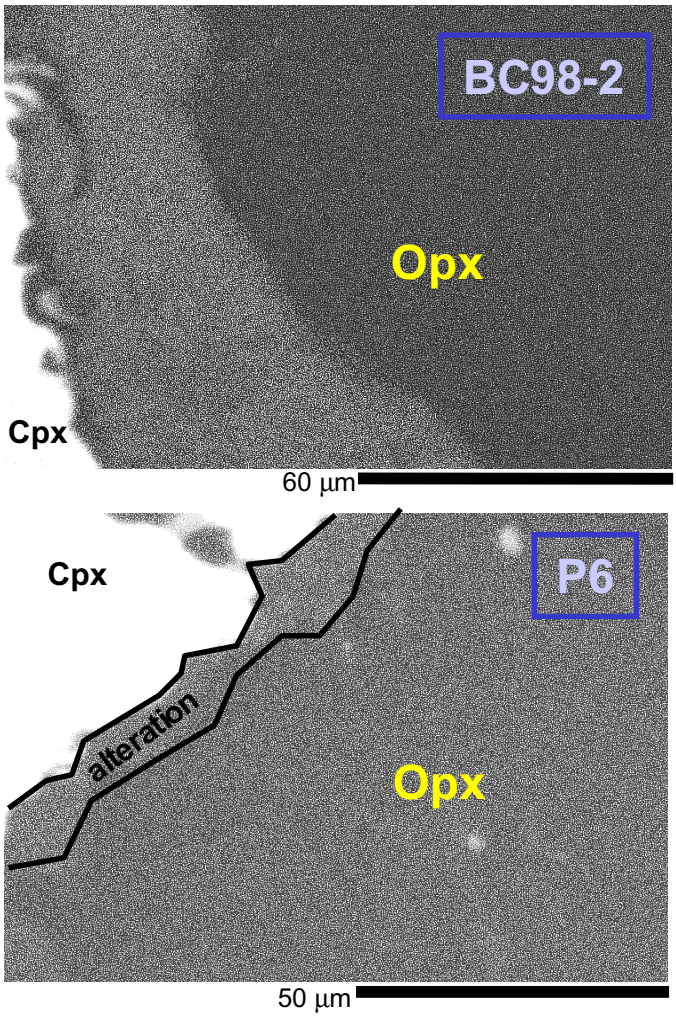

Figure 8. X ray image of relative variations in CaO content of orthopyroxenes (lighter regions are more CaO rich). Note the slightly enriched CaO rim in BC98-2 orthopyroxenes. On the scale of this measurement, zoning is not seen in P6 (compare with Figure 7).

inferred for Re/Os), the narrow range in $^{187}Os/^{188}Os$ requires that melt depletion occurred in the Phanerozoic. In contrast, the two shallow peridotites (BC98-2 and P2) have unradiogenic $^{187}Os/^{188}Os$ ratios, indicative of a Proterozoic melt extraction event. These latter two peridotites probably represent relicts of the original lithospheric mantle beneath the Sierra Nevada, which is Proterozoic, whereas the deeper, cooled peridotites are recent asthenospheric additions to the lithosphere.

[23] All of the peridotites carried by the Pleistocene Oak Creek basalt flow have $^{187}Os/^{188}Os$ ratios that lie within or very close to modern day asthenospheric values (0.122–0.130). However, because of the fertile nature of the Oak Creek peridotites (and hence near-chon-

dritic $^{187}Re/^{188}Os$), these Os isotopic data provide no strong time constraints on the timing of melt depletion, hence lithosphere formation.

5. Discussion

5.1. A Mesozoic Lithospheric Removal Event Beneath the Sierra Nevada

[24] The xenoliths carried in the Miocene Big Creek pipe reveal a lithosphere stratified in terms of age and thermal history. The deeper lithosphere (>45–60 km) is young and has cooled from >1100° to 700–800°C. The shallower portion (<45–60 km) is ancient and shows no evidence for cooling, and some samples show evidence for heating from <700° to 800–900°C. These observations suggest that any original Proterozoic lithospheric mantle deeper than 45–60 km depth (and up to at least 100 km, based on the highest equilibration pressures) has been removed or thinned and subsequently replaced by newly incorporated asthenospheric mantle. Thus, in late Miocene times, the shallowest portion is all that remains of the original Proterozoic lithosphere, and the deeper portion represents the newly accreted asthenosphere. In the ensuing paragraphs, we estimate when the deeper portion of the Sierran lithosphere was accreted, and whether this lithospheric thinning and rejuvenation event was due to extension or some form of lithospheric removal.

[25] Some time constraints can be placed on the event recorded by the late Miocene basalt-hosted Big Creek peridotites. While the Os isotopic data indicate that the deeper peridotites underwent melt depletion in the Phanerozoic, a more precise maximum bound on when this lithosphere formed can be had by estimating the amount of time needed to smooth out the diffusion profiles observed in the orthopyroxenes (Figures 7 and 10). We use the order of magnitude relationship between diffusion time (t) and diffusion distance (x), $t = x^2/D$, where D is the diffusion coefficient (m^2/s). From Figure 7, Ca diffusion length-scales in orthopyroxene are 0.2–0.3 mm. Assuming residence temperatures of ~800°C and a Ca diffusion coefficient in orthopyroxene at 800°C of $\sim 10^{-23}$ m^2/s [see *Griffin et al.*, 1996, and references therein], we estimate that such profiles should be erased within 100–300 Ma of their formation. Similarly, we find that the Al diffusion profiles at the contact between orthopyroxene and garnet lamellae (Figure 10) suggest a maximum elapsed time of ~150 Ma (assuming $D_{Al} = 6 \times 10^{-25}$ m^2/s at 800°C [*Smith and Barron*, 1991]). We conclude that lithospheric thinning must have occurred after 150 Ma in order for the zoning profiles to be preserved.

[26] If removal of lithospheric mantle is rapid enough that the overlying lithosphere remains cold during the process, the upwelling hot asthenosphere will cool against the overlying lithosphere, heating it in turn. This is what we observe in the Big Creek xenoliths. We interpret this stratification in thermal history and isotopic composition as evidence for lithospheric removal (delamination, foundering, etc.) instead of extensional thinning, as discussed in the next paragraph. Our data may also be consistent with thermal erosion of the Sierran lithosphere, provided that the upwelling asthenospheric mantle responsible for the thermal erosion eventually accreted to the base of the lithosphere.

[27] In contrast to the above observations, extensional thinning is a more gradual processes, which heats the lithosphere during thinning, resulting in elevated geotherms (Figure 2c). When thermal reequilibration occurs, both the lithosphere and the underlying asthenosphere must cool (Figure 2d). In these situations, one would not expect to see any correlation between thermal history, depth, and age of the litho-

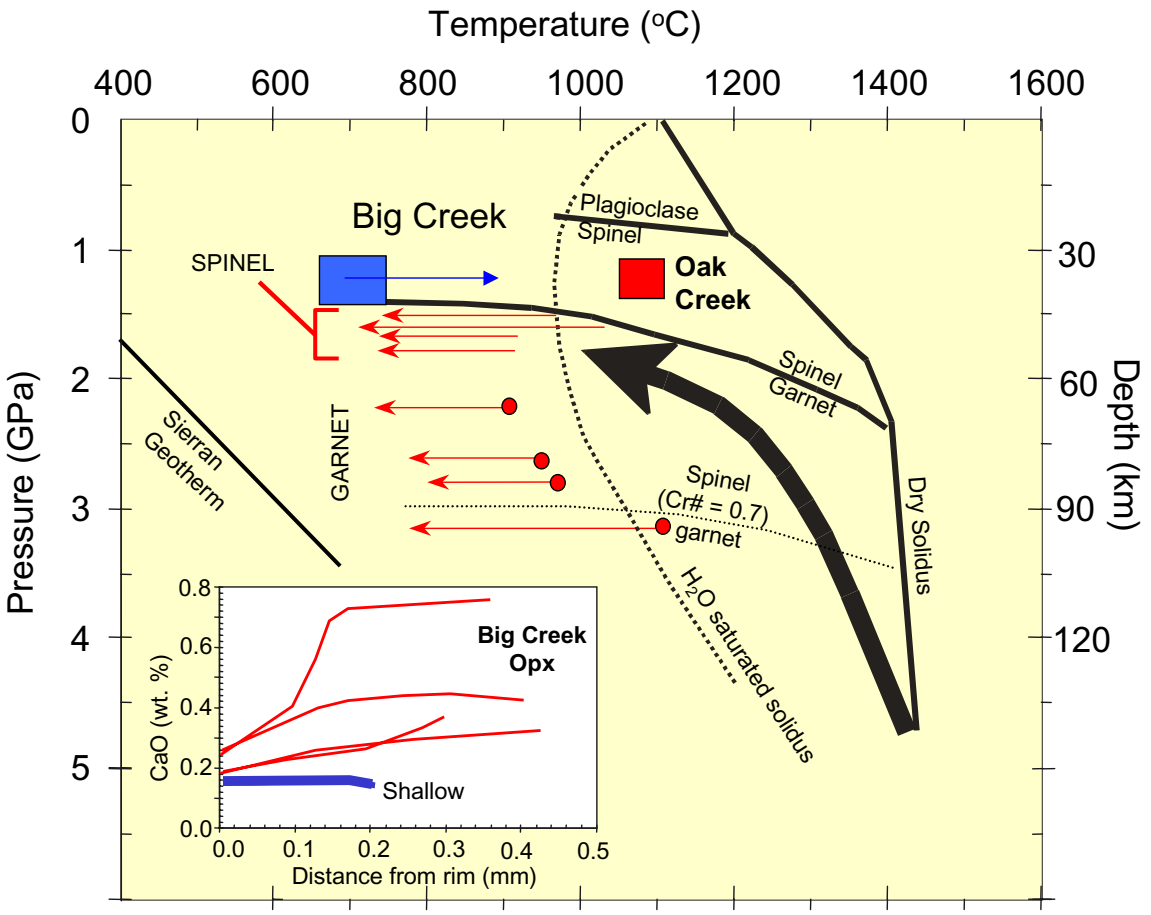

Figure 9. Pressure-temperature diagram showing results of thermobarometry. Arrows connect "peak" temperatures (based on CaO in orthopyroxene cores) to "final" temperatures (based on CaO content of orthopyroxene rims in contact with clinopyroxene). Pressures for garnet-bearing peridotites (arrows with circled ends) calculated from a garnet-orthopyroxene barometer [*Brey and Kohler*, 1990]. Pressures for spinel peridotites are constrained to be less than ~2 GPa (based on the absence of garnet and observed Cr # in spinel); their exact position on the diagram should not be taken literally. Oak Creek peridotites represented by red square; pressures for Oak Creek peridotites are constrained to be less than ~1.5 GPa based on the more aluminous nature of their spinels. Large arrow represents a possible *P-T* path that would account for the cooling history recorded in the Big Creek peridotites that show cooling. Dotted line represents the dry lherzolite solidus, with plagioclase-spinel and spinel-garnet transitions for fertile lherzolite. Higher Cr contents in spinel will depress transition to 2–3 GPa [*O'Neill*, 1981; *Girnis and Brey*, 1999]; dashed line represents spinel/garnet transition for spinel of Cr/(Cr + Al) = 0.60 [*Girnis and Brey*, 1999]. Sierran model geotherm based on a 41 mW/m^2 surface heat flow [*Lachenbruch and Sass*, 1977]. Inset shows a summary of CaO diffusion profiles in orthopyroxene (see Figure 7).

spheric mantle. Additional evidence against extension as the cause of pre-Miocene lithospheric removal comes from the fact that the only recognized extensional events in southwestern North America occurred in the middle to latest Proterozoic continental breakup [*Stewart*, 1972] and in the middle to late Cenozoic intracontinental extension in the Basin Range,

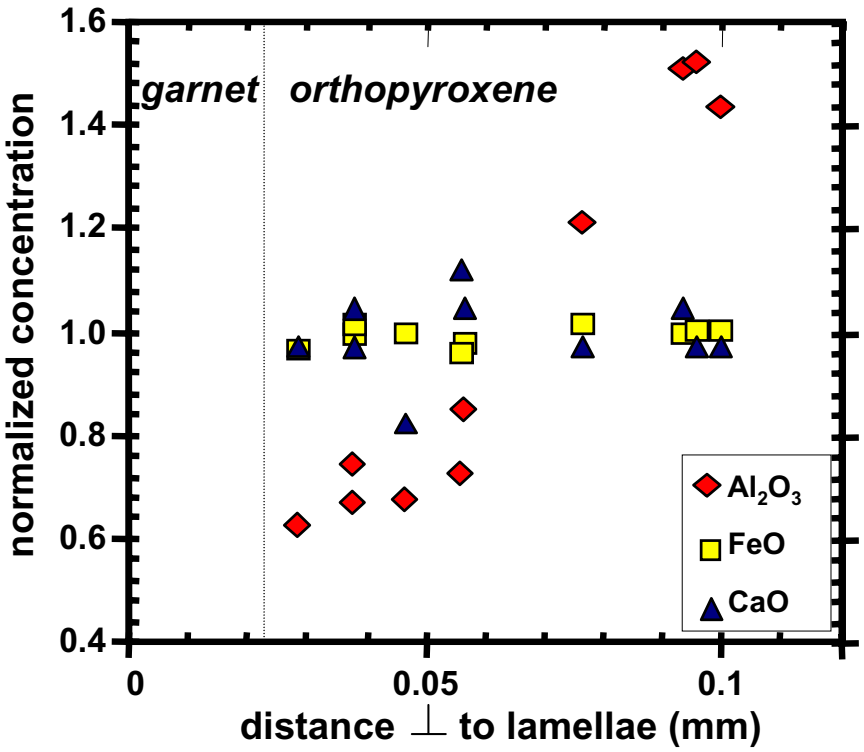

Figure 10. Electron microprobe analyses in an orthopyroxene lamella bounded by exsolved garnet lamellae (1026V). Only half of the diffusion profile is shown. Concentrations have been normalized to the average of all analyses in order to plot all elements on the same scale.

which peaked between 10–15 Ma ago [*Wernicke et al.*, 1988]. Thus the former occurred too early, while the latter occurred too recently to fit the time constraints discussed above.

[28] If our time constraints are robust, they place the hypothesized lithospheric removal event either in the Mesozoic or early Cenozoic, in which case lithospheric removal may have been associated with Mesozoic arc magmatism or early Cenozoic low-angle subduction. However, because it is generally believed that low-angle Cenozoic subduction resulted in the cessation of magmatism in the Sierra Nevada [*Dickinson and Snyder*, 1978] and because many of the Big Creek xenoliths appear to be residues of partial melting, we suggest that lithospheric removal most likely occurred during Mesozoic arc magmatism.

[29] Finally, the fact that a sliver of original Proterozoic lithospheric mantle still remained after the Mesozoic lithospheric removal event (as evidenced by the two "cold" samples from Big Creek with Proterozoic Os isotopic compositions) indicates that wholesale removal of the lithospheric mantle did not occur. This suggests that lithospheric removal did not occur by "mechanical" processes, such as delamination, insofar as existing models for delamination invoke wholesale removal of the lithospheric mantle and/or lower crust. It is

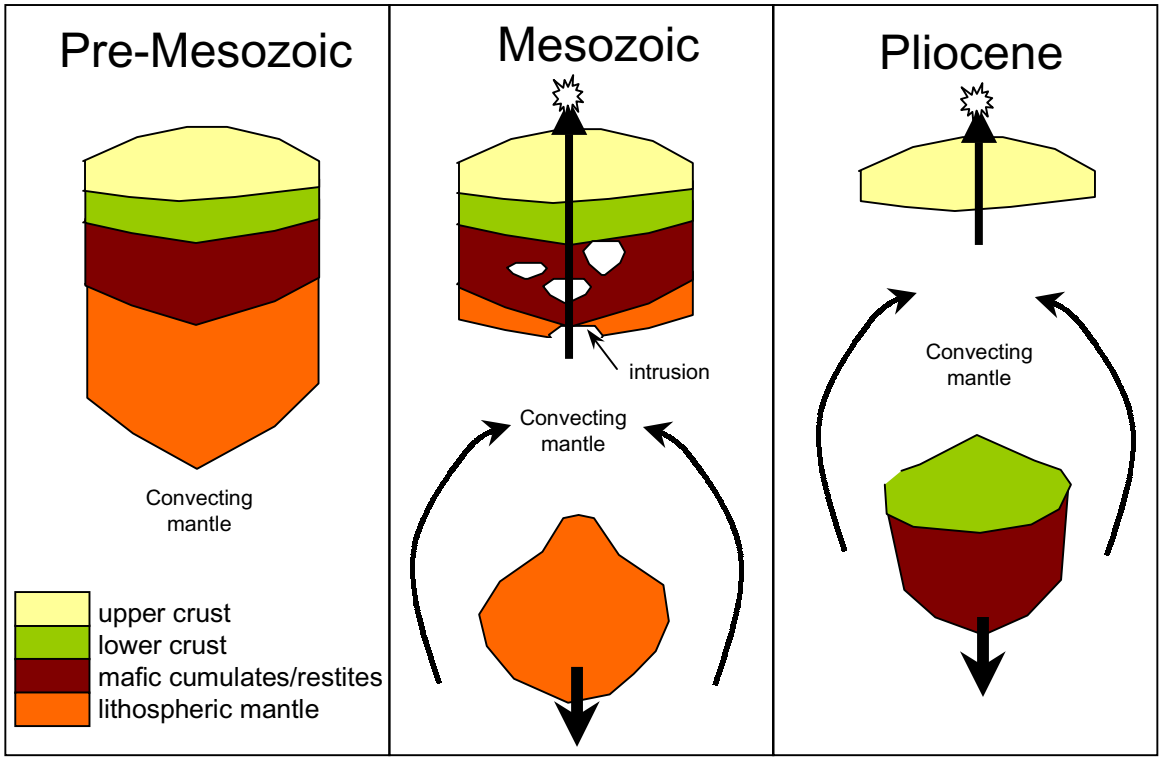

Figure 11. Schematic sequence of events describing the two-step scenario of lithospheric removal beneath the Sierra Nevada. Before the late Miocene, the lithospheric mantle, consisting of peridotitic material, is removed. This event is hypothesized to have occurred during the late Mesozoic or early Cenozoic. Sometime during the Pliocene, the mafic lower crust is also removed. This diagram is not meant to describe the actual mechanism.

instead more consistent with "fluid" styles of lithospheric removal, which result in the progressive removal of lithospheric mantle.

5.2. Late Cenozoic Thermal History

[30] The Pleistocene Oak Creek peridotites reveal a different chapter in the thermal evolution of the Sierran lithosphere. These peridotites have unzoned minerals that record hot temperatures (1000°–1100°C), although not hot enough to represent adiabatically ascending asthenospheric mantle, which would have temperatures of ~1300°C. As such, these peridotites probably represent fragments of the late Cenozoic Sierran lithospheric mantle.

[31] For reasons stated earlier, the Os isotopic compositions of the Pleistocene Oak Creek peridotites cannot be used to constrain the time of lithospheric formation. However, if most of the original Proterozoic lithospheric mantle was removed by the late Miocene (as suggested above), the Oak Creek xenoliths must also be young. If lithospheric removal occurred during a Mesozoic event, the Oak Creek peridotites represent post-Mesozoic lithospheric mantle, which may have formed in either of two ways: (1) the Oak Creek peridotites are fragments of the lithospheric mantle that was reheated after the hypothesized Mesozoic removal event or (2) they represent new (post-Miocene) lithosphere formed after slow-down of extension

and/or a late Cenozoic lithospheric removal event.

[32] The relatively fertile compositions of the Pleistocene Oak Creek peridotites contrast with the wide range in compositions found in the Miocen peridotite suite, suggesting that the Oak Creek peridotites do not represent simple reheating of the Miocene lithosphere. Additionally, reheating would have to occur within the time period bracketed by the age of Big Creek and Oak Creek eruptions (8 Ma). However, because the Oak Creek peridotites come from shallower than 45 km and the cooled Sierran lithosphere extended down to at least 100 km by the late Miocene, 8 Ma does not afford enough time for conductive reheating of this thickness of lithosphere.

[33] Circumstantial evidence suggests that Oak Creek peridotites represent new lithospheric mantle formed after a second lithosphere removal event or during slow-down of extension in the Pliocene. *Ducea and Saleeby* [1998b] observed that mafic lower crustal xenoliths were present in Miocene xenolith suites but absent in Pliocene and younger suites. They cited this as evidence for removal of mafic lower crust during the Pliocene. While the secular change in xenolith lithology could be a result of a biased sampling of the lithosphere (and this can never be completely ruled out), there are other lines of evidence that support their original contention. First the depths of origin of the Oak Creek peridotites (<45 km) overlap those calculated for garnet websterites (35–0 km) from Big Creek [*Mukhopadhyay and Manton*, 1994]. The latter are believed to be mafic cumulates or restites associated with Sierran magmatism because they preserve mineral isochron ages within error of the age of the batholith [*Ducea and Saleeby*, 1998c]. Provided that the Sierran lithosphere was not originally thin beneath the eastern Sierras, where Oak Creek is located, the overlap in depth suggests that the garnet websterites were displaced by the fertile Oak Creek peridotites during the Pliocene. This implies that the lithosphere thinned by at least ~50% between 8 Ma and the present, assuming that the lithospheric mantle formed after the Mesozoic removal event had grown to at least ~100 km (as determined from the Big Creek sample with the highest equilibration pressure).

[34] These observations are consistent with extension or rapid lithospheric removal. For example, a thinning factor of 50% is consistent with an estimate of ~200% or more Cenozoic crustal extension in the western Basin and Range [*Wernicke et al.*, 1988] and magmatic and isotopic evidence for 50% thinning of lithosphere beneath southeastern Nevada [*Daley and DePaolo*, 1992].

[35] Alternatively, the Oak Creek peridotite data are also consistent with a sudden removal of lower crust and underlying lithospheric mantle. High velocity anomalies at ~150–200 km depth beneath the western and southern Sierras may represent recently delaminated blobs [*Zandt and Carrigan*, 1993; *Jones et al.*, 1994]. In such a scenario, the Oak Creek peridotites would therefore represent hot asthenospheric mantle that upwelled after lithospheric removal. If so, the fact that the Oak Creek peridotites are still hot and show no evidence for cooling suggest that this lithospheric removal event was recent enough that significant thermal reequilibration has not yet occurred.

[36] If this late Cenozoic lithospheric thinning event is ascribed to lithospheric removal instead of extension, then the absence of any ancient lithospheric mantle and mafic lower crust in the Pliocene xenolith suites might indicate that lithospheric mantle and lower crust were removed wholesale, consistent with "mechanical" styles of lithospheric removal,

such as delamination. Regardless of whether the late Cenozoic thinning event was by delamination or extension, the Oak Creek peridotites indicate that the new lithospheric mantle accreted to the Sierran lithosphere during Mesozoic times was subsequently removed and replaced by even younger asthenospheric mantle. Two lithospheric removal events beneath the Sierra Nevada are thus implied (Figure 11).

6. Conclusions

[37] Peridotite xenoliths carried in late Miocene basalts from the central Sierra Nevada reveal that the Sierran lithosphere was vertically stratified in terms of age and thermal history. The shallow portion (<45–60 km) represents original, refractory Proterozoic lithospheric mantle and shows variable evidence for heating from <700° to 800°–900°C. The deeper portion (45–100 km) represents newly incorporated asthenospheric mantle and shows cooling from >1100° to 700°–800°C. Combined with various time constraints, these observations appear to be most consistent with a Mesozoic lithospheric removal event associated with Sierran arc magmatism. The form of this lithospheric removal event could have involved convective downwellings or thermal erosion. In either of these scenarios, the deeper xenoliths represent fragments of hot asthenospheric mantle that upwelled and cooled against the overlying cold lithosphere, which itself was heated, as represented by the shallow xenoliths.

[38] Fertile peridotite xenoliths carried in Pleistocene volcanics from the eastern Sierra Nevada have unzoned minerals recording hot temperatures (1000°–1100°C). These may represent new asthenospheric mantle incorporated into the lithosphere as a result of a slowing down of extension in the latest Cenozoic or as a result of a second lithospheric removal event. Regardless of their origin, the hot temperatures imply that thermal reequilibration associated with the aftermath of Mesozoic lithospheric removal was cut short in the Pliocene.

Acknowledgments

[39] Discussions with C. Conrad, P. F. Hoffman, M. Jull, and P. Molnar were valuable in honing our ideas regarding "delamination." We also thank M. Ducea, R. W. Carlson, J. T. Chesley, M. Handler, D. Hassler, S. B. Jacobsen, R. Kistler, A. Maloof, T. Plank, K. Yamashita, and Q.-Z. Yin for helpful discussions. M. Ducea and P. Molnar are thanked for insightful reviews, and M. Gurnis is thanked for efficient editorial handling. D. Lange (Harvard) and J. Donovan (U.C. Berkeley) are appreciated for help in electron microprobe analysis. S. Sorensen (Smithsonian) and R. Kistler (USGS) are thanked for donating portions of previously studied samples. This work was funded by the NSF. C.-T. Lee's fieldwork was supported by an NSF graduate fellowship, a Mineralogical Society of America Grant, and an ARCS Foundation Scholarship.

References

Bird, P., Continental delamination and the Colorado Plateau, *J. Geophys. Res.*, *84*, 7561–7571, 1979.

Bird, P., Formation of the Rocky Mountains, western United States: A continuum computer model, *Science*, *239*, 1501–1507, 1988.

Brey, G. P., and T. Kohler, Geothermobarometry in four-phase lherzolites, II, New thermobarometers, and practical assessment of existing thermobarometers, *J. Petrol.*, *31*, 1353–1378, 1990.

Conrad, C. P., and P. Molnar, The growth of Rayleigh-Taylor-type instabilities in the lithosphere for various rheological and density structures, *Geophys. J. Int.*, *129*, 95–112, 1997.

Daley, E. E., and D. J. DePaolo, Isotopic evidence for lithospheric thinning during extension: Southeastern Great Basin, *Geology*, *20*, 104–108, 1992.

Dickinson, W. R., and W. S. Snyder, Plate tectonics of the Laramide orogeny, in *Laramide folding associated with basement block faulting in the western United States*, edited by V. Matthews, *Geol Soc. Am. Mem.*, 355–366, 1978.

Dodge, F. C. W., J. P. Lockwood, and L. C. Calk, Fragments of the mantle and crust beneath the Sierra Nevada batholith: Xenoliths in a volcanic pipe near Big Creek, California, *Geol. Soc. Am. Bull.*, *100*, 938–947, 1988.

Ducea, M. N., and J. B. Saleeby, Buoyancy sources for a large, unrooted mountain range, the Sierra Nevada, Ca-

lifornia: Evidence from xenolith thermobarometry, *J. Geophys. Res.*, *101*, 8229–8244, 1996.

Ducea, M., and J. Saleeby, A case for delamination of the deep batholithic crust beneath the Sierra Nevada, California, in Integrated Earth and environmental evolution of the southwestern United States, Geol. Soc. Am. Spec. Vol., edited by G. Enrst and C. Nelson, pp. 273–288, Boulder, Colo., 1998a.

Ducea, M., and J. Saleeby, Crustal recycling beneath continental arcs: Silica-rich glass inclusions in ultramafic xenoliths from the Sierra Nevada, California, *Earth Planet. Sci. Lett.*, *156*, 101–116, 1998b.

Ducea, M. N., and J. B. Saleeby, The age and origin of a thick mafic-ultramafic keel from beneath the Sierra Nevada batholith, *Contrib. Mineral. Petrol.*, *133*, 169–185, 1998c.

Farmer, G. L., F. V. Perry, S. Semken, B. Crowe, D. Curtis, and D. J. DePaolo, Isotopic evidence on the structure and origin of subcontinental lithospheric mantle in southern Nevada, *J. Geophys. Res.*, *94*, 7885–7898, 1989.

Feldstein, S. N., and R. A. Lange, Pliocene potassic magmas from the Kings River region, Sierra Nevada, California: Evidence for melting of a subduction-modified mantle, *J. Petrol.*, *40*, 1301–1320, 1999.

Girnis, A. V., and G. P. Brey, Garnet-spinel-olivine-orthopyroxene equilibria in the FeO-MgO-Al_2O_3-SiO_2-Cr_2O_3 system, II, Thermodynamic analysis, *Eur. J. Mineral.*, *11*, 619–636, 1999.

Griffin, W. L., D. Smith, C. G. Ryan, S. Y. O'Reilly, and T. T. Win, Trace-element zoning in mantle minerals: Metasomatism and thermal events in the upper mantle, *Can. Mineral.*, *34*, 1179–1193, 1996.

Harley, S. L., An experimental study of the partitioning of Fe and Mg between garnet and orthopyroxene, *Contrib. Mineral. Petrol.*, *86*, 359–373, 1984.

Harley, S. L., and D. H. Green, Garnet-orthopyroxene barometry for granulites and peridotites, *Nature*, *300*, 697–701, 1982.

Houseman, G. A., and P. A. Molnar, Gravitational (Rayleigh-Taylor) instability of a layer with non-linear viscosity and convective thinning of continental lithosphere, *Geophys. J. Inter.*, *128*, 125–150, 1997.

Houseman, G. A., D. P. McKenzie, and P. Molnar, Convective instability of a thickened boundary layer and its relevance for the thermal evolution of continental convergent belts, *J. Geophys. Res.*, *86*, 6115–6132, 1981.

Jarvis, G. T., and D. P. McKenzie, Sedimentary basin formation with finite extension rates, *Earth Planet. Sci. Lett.*, *48*, 42–52, 1980.

Jones, C. H., H. Kanamori, and S. W. Roecker, Missing roots and mantle "drips": Regional Pn and telseismic arrival times in the southern Sierra Nevada and vicinity, California, *J. Geophys. Res.*, *99*, 4567–4601, 1994.

Kay, R. W., and S. M. Kay, Delamination and delamination magmatism, *Tectonophys*, *219*, 177–189, 1993.

Kistler, R. W., Two different lithosphere types in the Sierra Nevada, California, in *The Nature and Origin of Cordilleran Magmatism*, edited by J. L. Anderson, pp. 271–281, Geol. Soc. of Am., Boulder, Colo., 1990.

Lachenbruch, A. H., and J. H. Sass, Heat flow in the United States and the thermal regime of the crust, in *The Earth's Crust, Its Nature and Physical Properties*, *Geophys. Monogr. Ser.*, vol. 20, edited by J. G. Heacock, pp. 625–675, AGU, Washington, D. C., 1977.

Lee, C.-T., Q.-Z. Yin, R. L. Rudnick, J. T. Chesley, and S. B. Jacobsen, Re-Os isotopic evidence for pre-Miocene delamination of lithospheric mantle beneath the Sierra Nevada, California, *Science*, *289*, 1912–1916, 2000.

McKenzie, D., and R. K. O'Nions, Mantle reservoirs and ocean island basalts, *Nature*, *301*, 229–231, 1983.

Moore, J. G., and F. C. W. Dodge, Late Cenozoic volcanic rocks of the southern Sierra Nevada, California, 1, Geology and petrology: Summary, *Geol. Soc. Am. Bull.*, *91*, 515–518, 1980.

Mukhopadhyay, B., and W. I. Manton, Upper mantle fragments from beneath the Sierra Nevada batholith-partial fusion, fractional crystallization and metasomatism in subduction-related ancient lithosphere, *J. Petrol.*, *35*, 1418–1450, 1994.

O'Neill, H. S. C., The transition between spinel lherzolite and garnet lherzolite, and its use as a geobarometer, *Contrib. Mineral. Petrol.*, *77*, 185–194, 1981.

Ranalli, G., Rheology of the Earth, 2nd ed., 413 pp., Chapman and Hall, New York, 1995.

Rudnick, R. L., Making continental crust, *Nature*, *378*, 571–578, 1995.

Ruppert, S., M. M. Fliedner, and G. Zandt, Thin crust and active upper mantle beneath the southern Sierra Nevada in the western United States, *Tectonophys.*, *286*, 237–252, 1998.

Smith, D., and B. R. Barron, Pyroxene-garnet equilibration during cooling in the mantle, *Am. Mineral.*, *76*, 1950–1963, 1991.

Stewart, J. H., Initial deposits in the Cordilleran Geosyncline: Evidence of a late Precambrian (<850 m.y.) continental separation, *Geol. Soc. Am. Bull.*, *83*, 1345–1360, 1972.

Wernicke, B., R. Clayton, M. Ducea, C. H. Jones, S. Park, S. Ruppert, J. Saleeby, J. K. Snow, L. Squires, M. Fliedner, G. Jiracek, R. Keller, S. Klemperer, J. Luetgert, P. Malin, K. Miller, W. Mooney, H. Oliver,

and R. Phinney, Origin of high mountains in the continents: the southern Sierra Nevada, *Science*, *271*, 190–193, 1996.

Wernicke, B., G. J. Axen, and J. K. Snow, Basin and Range extensional tectonics at the latitude of Las Vegas, Nevada, *Geol. Soc. Am. Bull.*, *100*, 1738–1757, 1988.

Zandt, G., and C. R. Carrigan, Small-scale convective instability and upper mantle viscosity under California, *Science*, *261*, 460–463, 1993.